Inorganica Chimica Acta, 106 (1985) 101–108

Crystal Structure and Magnetic Properties of a Tetramer with a Step-like $Cu_4N_4O_2$ Core containing Asymmetric Bridged Dimeric Subunits related to the Hemocyanin Copper Active Site

JÜRGEN LORÖSCH, HELMUT PAULUS and WOLFGANG HAASE*

Institut für Physikalische Chemie, Technische Hochschule Darmstadt, Petersenstrasse 20, 6100 Darmstadt, F.R.G.

Received September 6, 1984

Abstract

The Cu(II)-derivate of the macrocycle L derived from 2-hydroxy-5-methylisophthalaldehyde and 3-dimethylamino-1-propylamine forms tetranuclear $\{[LCu_2(N_3)_3](ClO_4)_2\}_2$ units. The crystal structure determined by X-ray crystallography is based on a step-like $Cu_4N_4O_2$-core with interdimeric $\mu(1)$-azido bridging. The tetramer is formed from two dimeric subunits which are connected by a center of symmetry. The subunits are asymmetric bridged dimeric complexes with a phenolate and a $\mu(1)$-azido bridge. The coordination polyhedra around the two copper atoms are 4 + 2 and 4 + 1 including one coordinating perchlorate ion.

The magnetic susceptibility of the complex has been measured in the temperature range 4.2 K to 315.6 K. The theoretical analysis using models for tetrameric and dimeric interactions revealed only a small interdimeric interaction. The magnetic exchange coupling of the asymmetric bridged dimeric unit ($2J = -528$ cm^{-1}) is comparable to that of known di-oxygen bridged dimers. The results are related to the magnetic behaviour of the asymmetric bridges found in the binuclear copper sites in hemocyanin.

Infrared measurements have been taken and there is a discussion of the asymmetric vibrations of the three different azido-groups.

Introduction

The only known dinuclear copper(II) site in proteins has been found in respiratory proteins (hemocyanin) and oxidases (*e.g.* laccase, ceruloplasmin) [1]. The structural picture of this active site has been particularly studied in the case of hemocyanin by vibrational [2, 3], chemical [4] and electronic [4, 5] techniques indicating endogenous and exogenous bridging ligands between the two coppers. The exogenous ligand is O_2^{2-} in oxyhemocyanin and N_3^-, CN^-, etc. in methemocyanin derivatives.

The endogenous bridge is unknown but an O-atom donor, tyrosine or oxo oxygen atoms have been proposed [1]. EXAFS data show Cu–Cu distances of about 3.6 Å in oxyhemocyanin and 3.45 Å in methemocyanin derivates leading to bridging angles of about 130°–140° at the endogenous ligand [6].

Magnetic investigations showed strong antiferromagnetic coupling between the two copper(II)-ions ($|2J| > 550$ cm^{-1}) resulting in diamagnetism [7].

To understand the magnetic behaviour of this native dinuclear copper(II) site it is important to appreciate the role of the bridging angle Cu–O–Cu of about 130°–140° and the presence of asymmetric bridges.

Angles of about 130°–140° at the bridging oxygen are known only for a few examples involving mono- or unsymmetric bridges [8–11]. Double bridged copper(II)-dimers having hydroxo-, alkoxo- or phenoxo bridges often have strong antiferromagnetic coupling for Cu–O–Cu angles between 100° and 105° and Cu–Cu distances of about 3.0 Å [12, 13].

Unsymmetric bridged dimers are widely known [8, 14–17] using five- and seven-dentate macrocyclic ligands but a connection between structure and magnetic behaviour has not been shown. In this report we describe the structural and magnetic behaviour of a tetranuclear copper(II) complex. The dimeric subunit has a phenolate and an azide bridge in which the azide is bound end-on. The understanding of the magnetic exchange of this compound is of great interest because dimers bridged symmetrically by end-on bound azide-ions yield ferromagnetic coupling [18, 19] while oxygen-bridged dimers are strongly antiferromagnetically coupled [13] in the range of observed bridging angles of about 103°.

Experimental

Preparation

The dialdehyde 2-hydroxy-5-methylisophthalaldehyde was prepared according to the method described by Ullmann and Brittner [20]. A solution of 2-hydroxy-5-methylisophthalaldehyde (0.66 g, 4.0

*Author to whom correspondence should be addressed.

0020-1693/85/$3.30

TABLE I. Data Collection and Processing Parameters

Molecular formula	$C_{19}H_{33}N_{13}O_9Cl_2Cu_2 \times 1/2CH_3OH$
Molecular weight	805.16
Cell constants	$a = 14.104(2)$ Å
	$b = 12.199(2)$ Å
	$c = 10.908(2)$ Å
	$\alpha = 83.79(1)°$
	$\beta = 74.19(1)°$
	$\gamma = 65.32(1)°$
	$V = 1640.59$ Å^3
	$Z = 2$
D_m (by flotation)	1.61(2) g/cm^3
D_c	1.623 g/cm^3
Space group	$P\bar{1}$
Radiation	graphite-monochromatized
	MoK_α-radiation, $\lambda = 0.71069$ Å
Absorption coefficient	14.54 cm^{-1}
$F(000)$	814
Scan type	$\omega: 2\theta = 1:1$
Scan range	$6 \leqslant 2\theta \leqslant 45°$
Intensity variations	<3%
Unique data measured	4278
Observed data with $\|F_o\| > 3\sigma(\|F_o\|)$	3297
$R = \Sigma\|\|F_o\| - \|F_c\|\|/\Sigma\|F_o\|$	0.065

mmol) in methanol (20 ml) was reacted with 3-dimethylamino-1-propylamine (0.82 g, 8.0 mmol). The resulting orange solution was stirred for 15 min and $Cu(ClO_4)_2 \cdot 6H_2O$ (2.96 g, 8.0 mmol) was added slowly. Upon slow addition of NaN_3 (0.26 g, 4.0 mmol) a greenish brown precipitate was formed immediately. The solid was collected and recrystallized from methanol. Upon standing dark brown needle-like crystals were obtained. The crystals were vacuum-dried at 60 °C; m.p. 192°–194 °C. Elemental analysis results (%) for the crystalline product of empirical formula $C_{19}H_{33}N_{13}O_9Cl_2Cu_2 \cdot 1/2CH_3OH$ were as follows, with calculated values in parenthesis: C 29.21(29.09); H 4.30(4.43); N 22.17(22.62).

X-Ray Crystallography

A needle-like crystal of approximate dimensions 0.08 × 0.12 × 0.5 mm was measured on a computer controlled Stoe Stadi 4 four-circle-diffractometer system. The cell dimensions were obtained from least-squares refinement of the 2θ values of 70 strong reflections. The intensity data were corrected for Lorentz, polarization and absorption effects. The pertinent crystallographic data are summarized in Table I. Intensity statistics strongly favoured space group $P1$ and the positions of the two copper atoms were derived by direct methods using MULTAN 80 [21]. All 45 non-hydrogen atoms in the asymmetric unit were located after several Fourier syntheses, ΔF synthesis and successive least-squares cycles. After least-squares refinement using isotropic (R = 0.134) and anisotropic (R = 0.085) temperature factors all C-bound H atoms were geometrically generated (C–H distance fixed at 1.08 Å) and isotropic thermal parameters assigned.

The resulting ΔF map revealed two peaks corresponding to a solvent molecule of CH_3OH for which a site occupation factor of 0.5 was calculated. The final difference map was essentially flat, with residual extrema lying between 0.62 and –0.59 eÅ^{-3}. All the atomic scattering factors were taken from 'International Tables for X-ray Crystallography' [22] and ref. [23].

The crystal structure was determined and refined by use of a minicomputer program package developed by STOE & Cie., Darmstadt. The computer was a Data General Eclipse S/140 (256 kByte memory) at the application laboratory of STOE & Cie., Darmstadt. The final positional and thermal parameters with their estimated standard deviations are listed in Table II. The F_o/F_c lists, anisotropic temperature factors, and H-atom positional parameters are available on request from the authors.

Magnetic and Infrared Measurements

The magnetic susceptibility was recorded by the Faraday method as described previously [24] at *ca.* 10 kG(1T) in the temperature range 4.2 to 315.6 K. Experimental susceptibility data were corrected for underlying diamagnetism using Pascal's increments [25] and for temperature-independent paramagnetism. The calculation of the theoretical $\chi(T)$ curve was performed on a IBM 370/168 computer on the Technische Hochschule Darmstadt.

TABLE II. Atomic Positional Parameters and Equivalent Temperature Factors (Å^2) for all Non-hydrogen Atoms with e.s.d.s in Parentheses; $B_{eq} = \frac{8}{3}\pi^2(U_{11} + U_{22} + U_{33})$.

Atom	*x/a*	*y/b*	*z/c*	B_{eq}
Cu1	0.4535(1)	0.9270(1)	0.6428(1)	3.02
Cu2	0.6274(1)	0.7624(1)	0.4180(1)	3.35
C1	0.2213(10)	0.9032(9)	0.2262(8)	7.8
C2	0.2803(12)	0.7052(9)	0.1360(10)	5.0
N1	0.2833(6)	0.8275(6)	1.1129(6)	5.4
C3	0.2447(6)	0.8815(6)	0.9972(7)	3.9
C4	0.2705(6)	0.9899(6)	0.9502(6)	3.4
C5	0.2366(5)	1.0368(6)	0.8264(6)	2.9
N2	0.3037(4)	0.9484(5)	0.7210(5)	3.0
C6	0.2581(6)	0.8902(6)	0.6870(7)	3.5
O1	0.4756(3)	0.8034(4)	0.5211(4)	3.2
C7	0.4087(6)	0.7534(6)	0.5157(6)	3.0
C8	0.3026(6)	0.7950(6)	0.5939(6)	3.0
C9	0.2339(6)	0.7430(7)	0.5841(7)	3.8
C10	0.2647(7)	0.6472(7)	0.5036(7)	4.3
C11	0.1883(7)	0.5930(8)	0.4933(8)	6.2
C12	0.3705(7)	0.6054(7)	0.4277(7)	4.1
C13	0.4420(6)	0.6583(6)	0.4293(6)	3.2
C14	0.5454(6)	0.6074(6)	0.3398(7)	3.9
N3	0.6236(5)	0.6398(5)	0.3176(6)	3.5
C15	0.7180(6)	0.5732(6)	0.2126(7)	3.9
C16	0.7245(6)	0.6495(7)	0.0931(7)	4.0
C17	0.8123(7)	0.5717(7)	−0.0113(8)	4.6
N4	0.8356(8)	0.6230(8)	0.8664(7)	7.1
C18	0.7790(8)	0.7354(8)	−0.1754(9)	6.3
C19	0.9197(8)	0.5371(9)	0.7679(8)	6.2
N5	0.4418(5)	1.0693(5)	0.7255(6)	3.7
N6	0.4957(6)	1.0766(6)	0.7876(7)	4.6
N7	0.5464(8)	1.0873(9)	0.8497(10)	10.5
N8	0.6026(5)	0.8858(5)	0.5397(6)	3.9
N9	0.6686(6)	0.9133(6)	0.5636(6)	3.8
N10	0.7298(7)	0.9449(7)	0.5820(8)	6.6
N11	0.7815(6)	0.7084(7)	0.3565(7)	4.8
N12	0.8422(7)	0.6984(8)	0.4104(8)	6.0
N13	0.9072(9)	0.6822(14)	0.4628(13)	14.6
C11	0.5363(2)	0.6598(2)	0.8410(3)	6.4
O2	0.4582(5)	0.6356(6)	0.8050(7)	8.1
O3	0.5226(5)	0.7798(5)	0.8164(7)	8.0
O4	0.6359(6)	0.5821(8)	0.7913(13)	16.2
O5	0.5197(10)	0.6519(10)	0.9795(10)	18.6
C12	1.0338(2)	0.7642(2)	−0.0767(3)	5.5
O6	1.1437(5)	0.7094(6)	−0.0925(7)	7.8
O7	0.9704(6)	0.7258(7)	0.0194(8)	10.2
O8	1.0029(6)	0.8822(7)	−0.0800(13)	14.4
O9	1.0174(10)	0.7305(17)	−0.1858(11)	26.9
OM	0.0129(18)	0.1159(21)	0.6222(21)	15.8
CM	0.0167(29)	0.0592(30)	0.5098(27)	15.8

Infrared spectra in the region 4000–200 cm^{-1} were recorded on a Perkin Elmer 325 spectrophotometer with KBr pellets.

Results and Discussion

Description of the Structure

Binuclear $(Cu_2(N_3)_3L)^{2+}$-cations form subunits which are represented in Fig. 1. The step-like structure of the tetramer is formed by two binuclear subunits which are inverted by a center of symmetry in (1/2 1 1/2) resulting in C_i-symmetry. The tetramer is shown in Fig. 2 including two coordinating perchlorate groups. Selected bond distances and angles are given in Table III.

Step-like tetramers have been presented in the literature [26–29] but to our knowledge it is

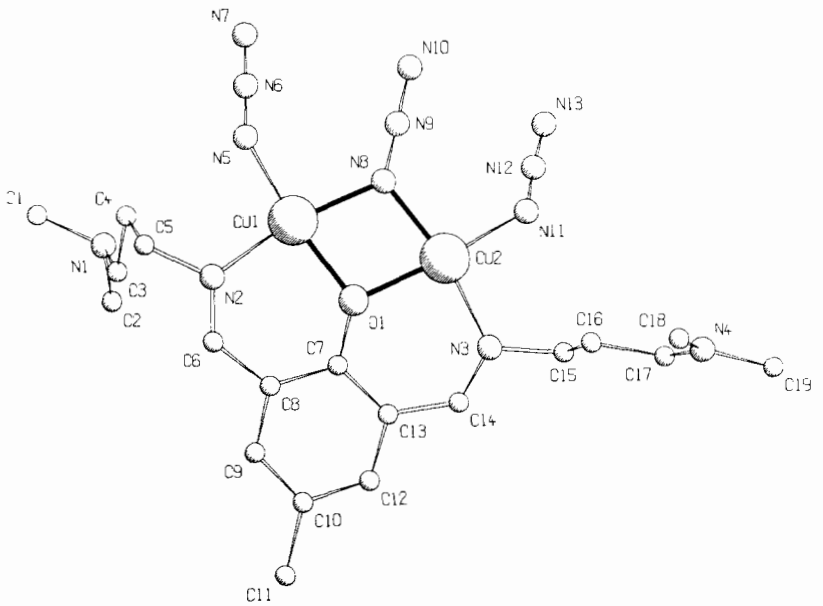

Fig. 1. Perspective view of the dimeric subunit.

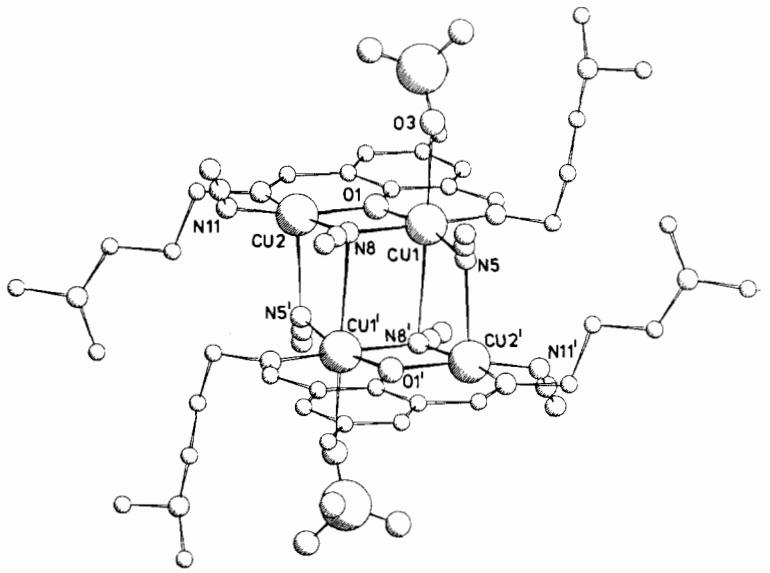

Fig. 2. Tetrameric molecular structure illustrating the $Cu_4N_4O_2$ core.

the first time that such a tetramer having $\mu(1)$-azido-bridges has been reported.

The macrocycle L is a double Schiff base acting as a tridentate ligand. The phenolate oxygen bridges the two copper atoms while the two imino nitrogens each coordinate to the copper atoms leading to two six-membered chelate rings which are crystallographically different. Normally the macrocycle L acts as a five-dentate ligand [14–16]. In our case the amino nitrogens N1 and N4 are replaced as coordinating positions by two azido-groups binding to the copper atoms. The other bridge in the binuclear subunit is formed by a third azido-group resulting in an asymmetric dimer bridged by the phenolate oxygen O1 and the azido-nitrogen N8. So each copper atom is coordinated in a square planar CuN_3O-sphere.

The different Cu–O distances are comparable (mean value 1.995(5) Å). The copper–imino nitrogen distances (mean value 1.969(6) Å) and the copper–azido nitrogen distances (mean value 1.972(7) Å) are the same within experimental error. Only the Cu2–N11 distance differs remarkably (see Table III).

TABLE III. Selected Bond Distances (Å) and Bond Angles (°) with e.s.d.s in Parentheses.

Cu1–Cu2	3.120(1)		
Cu1–Cu1′	3.623(1)		
Cu2–Cu1′	3.516(1)		
Cu2–Cu2′	5.573(1)		
Cu1–O1	1.987(5)	Cu2–O1	2.003(4)
Cu1–N2	1.965(6)	Cu2–N3	1.973(7)
Cu1–N5	1.969(7)	Cu2–N11	1.927(7)
Cu1–N8	1.973(6)	Cu2–N8	1.972(7)
Cu1–N8′	2.858(6)	Cu2–N5′	2.466(7)
Cu1–O3	2.563(7)		
N2–C6	1.275(12)	N5–N6	1.181(13)
C6–C8	1.440(10)	N6–N7	1.161(16)
O1–C7	1.336(11)	N8–N9	1.208(12)
C13–C14	1.437(9)	N9–N10	1.150(14)
N3–C14	1.277(12)	N11–N12	1.125(14)
		N12–N13	1.148(18)
Cu1–O1–Cu2	102.9(3)		
Cu1–N8–Cu2	104.5(4)		
O1–Cu1–N2	92.4(2)	O1–Cu2–N3	92.3(2)
O1–Cu1–N5	166.1(2)	O1–Cu2–N11	166.5(3)
O1–Cu1–N8	76.5(3)	O1–Cu2–N8	76.1(2)
N2–Cu1–N5	95.2(3)	N3–Cu2–N11	92.8(3)
N2–Cu1–N8	168.8(3)	N3–Cu2–N8	168.3(3)
N5–Cu1–N8	95.4(3)	N11–Cu2–N8	98.1(3)
C1–N1–C2	110.0(7)	C17–N4–C18	128.1(7)
C1–N1–C3	112.9(6)	C17–N4–C19	114.9(7)
C2–N1–C3	109.6(9)	C18–N4–C19	116.1(7)
N5–N6–N7	177.8(8)		
N8–N9–N10	176.2(8)		
N11–N12–N13	176.4(1.2)		

The atoms of the coordinating part of the macrocyclic ligand including the phenolate and the two chelate rings are situated in a nearly perfect plane with a maximum deviation from the mean plane of 0.06 Å. This reflects the aromatic character of the chelate ring system. All distances and angles of the ligand show normal values. The two outer azido-groups are found within a plane too (max. deviation 0.06 Å) having a dihedral angle to the planar part of the ligand L of 38.54°.

Two dimeric subunits inverted by a center of symmetry form a tetrameric molecule by coordinating N8 to Cu1 and N5 to Cu2 between the binuclear units resulting in interdimeric azide bridging. Four-membered rings of Cu1–N8–Cu1′–N8′, Cu1–N5–Cu2′–N8′ and the centrosymmetric one are formed (′: $1-x, 2-y, 1-z$). A step-like $Cu_4N_4O_2$ core represented in Fig. 2 results. The value for the interdimeric Cu1–N8′ distance (2.858(6) Å) was found to be significantly larger than the Cu2–N5′ distance (2.466(7) Å). This can be explained by the fact that Cu1 is coordinated additionally in a sixth position to an oxygen atom of the perchlorate group (Cu1–O3 2.563(7) Å). So the coordination polyhedron of Cu1 can be described as 4 + 2 having a square planar basis plane with two additional ligands perpendicular to this plane and more elongated. The coordination polyhedron around Cu2 can be assigned as 4 + 1 forming a distorted tetragonal pyramid with the N5′ atom at its apex. Both copper atoms are shifted above their base planes. Cu1 was found to have moved 0.13 Å towards O3 and Cu2 to have shifted 0.12 Å towards N5′.

Inspection of our molecule reveals three kinds of azido groups. The azido group N11–N12–N13 has been found to bind terminally to Cu2, while the group N5–N6–N7 forms a $\mu_2(1)$ bridge between two copper atoms. This type of bridge is well known and contains equivalent Cu–N distances. The third group N8–N9–N10 forms a $\mu_3(1)$ bridge which means that N8 is coordinated to three copper atoms. This type of azido-bridging is reported here for the first time. In agreement with known data [18, 30] we found larger Cu–N-distances involving the bridging azido-groups than the terminal ones (see Table III). The azido-group forming the $\mu_3(1)$ bridge shows an asymmetry of $\Delta d = 0.058(26)$ Å in the different N–N distances with the shorter N–N bond being remote from the metal atom, which is comparable to literature data [18, 30–32]. The other two azido-groups show symmetry for the different N–N bonds within experimental error. The results are in agreement with known data which show the terminal bonded azido-groups to be more symmetric than the bridging ones. All $Cu-N_\alpha-N_\beta$-angles are found to be rather similar between 126.1° and 129.4° (see Table III).

The tetrameric molecule is a fourfold positively charged cation. Inspection of the coordination around the amino nitrogens N1 and N4 shows a tendency to tetrahedral arrangement. So we assume positive charges at the amino nitrogen atoms including supplementary N–H-bonds. In Fig. 3 a projection along the crystallographic [*1 1 1*] line of selected atoms of the tetrameric molecule is presented. Because the elementary cell contains only one tetrameric unit, the molecules form layers perpendicular to each of the three elementary cell directions. The second perchlorate ion found in the elementary cell performs no bonding contact to atoms of the cation. So this perchlorate cation is situated in a separate place leading to internal rotations of this group which could explain the high standard deviation for the positional parameters. The same is true for the solvent molecules of methanol which are half positioned in two different places.

Magnetic Properties

The magnetic susceptibility of the crystalline complex has been measured in the temperature range 4.2 to 315.6 K. With increasing temperature the magnetic susceptibility decreases slightly at first

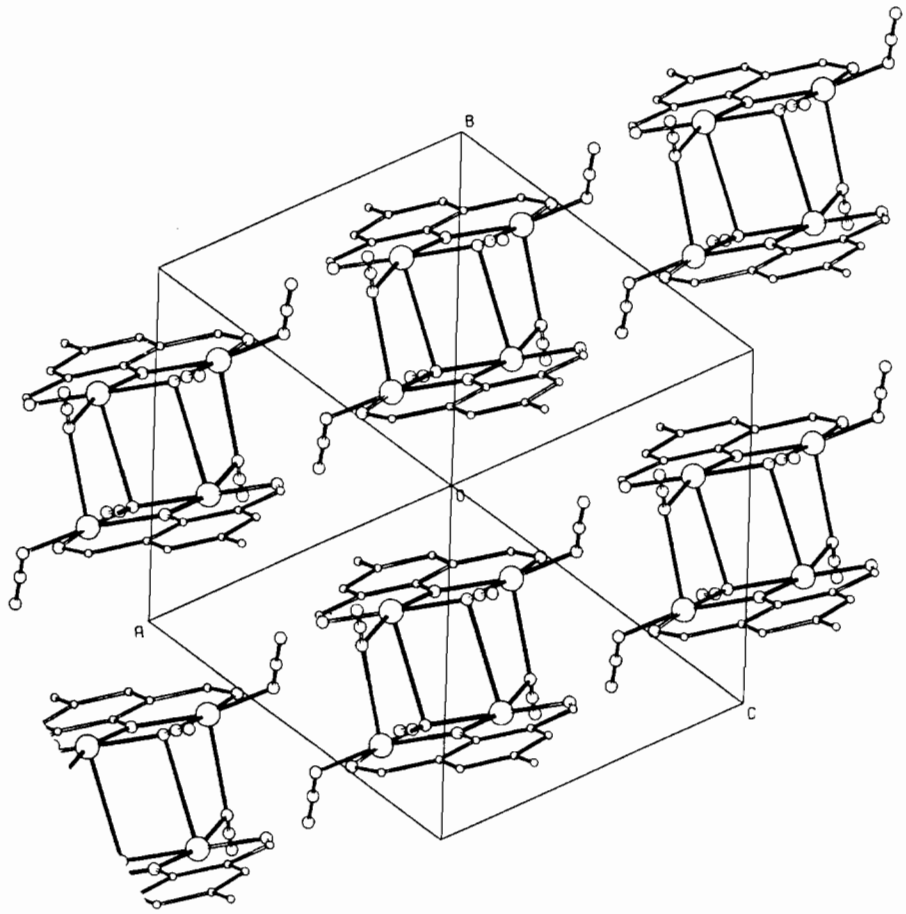

Fig. 3. Crystal structure of the title compound projected perpendicular to the crystallographic [*1 1 1*] line. The side chains, perchlorate ions and solvent molecules have been omitted for clarity.

because of a few paramagnetic impurities. At about 70 K the magnetic susceptibility begins to increase without reaching a maximum in the studied temperature range. This can be interpreted as an antiferromagnetic coupling.

A quantitative theoretical analysis of the magnetic behaviour of the tetrameric cluster is given using the isotropic Heisenberg-Dirac-van Vleck (HDvV) model. This Hamiltonian is

$$\mathcal{H} = -2 \sum_{i<j} J_{ij} S_i S_j \qquad (1)$$

J_{ij} is the exchange integral between the magnetic centres i and j. There are two kinds of interpretation:

– The tetrameric copper arrangement shows C_i-symmetry. Therefore it is possible to describe the magnetic behaviour by four different exchange integrals (see Fig. 4).

The Hamiltonian then becomes as in eqn. (2):

$$\mathcal{H} = -2J_{12}(S_1S_2 + S_1'S_2') - 2J_{11}'(S_1S_1') - 2J_{12}'(S_1S_2' + S_2S_1') - 2J_{22}'(S_2S_2') \qquad (2)$$

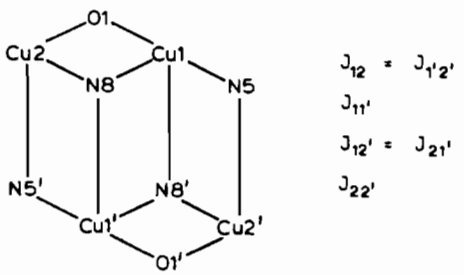

Fig. 4. Principal structure of the $Cu_4N_4O_2$ core with C_i symmetry and relations between the exchange integrals.

The equation used for calculating the magnetic susceptibility has been evaluated, *e.g.* by Hatfield and Inman [33].

– Assuming no interdimeric interaction the magnetic behaviour of the tetramer can be interpreted as exchange coupling of discrete dimers. For theoretical description we used the well-known Bleaney-Bowers equation [34].

The exchange integrals J_{ij}, χ_{para} from the paramagnetic impurities and the temperature independent

paramagnetism N_α were fitted by least squares techniques using eqn. (3):

$$\chi_{exp} = (1 - x)\chi_{Mol} + x\chi_{para} + \chi_{N\alpha} + \chi_{dia} \quad (3)$$

The function minimized was $|\chi_{exp} - \chi_{calc}|/\chi_{exp}$. In the applied calculation procedure the J-value has been found to depend on the g-factor and on the paramagnetic impurities. So the g-factor was kept constant at 2.20 corresponding to the best known dimers. During refinement using the tetrameric model we assumed J_{22}' to be zero because of the long pathway described by this interaction.

Table IV shows the comparison between the two proposed models assuming dimeric as well as tetrameric interaction.

TABLE IV. Comparison of the Exchange Integrals (cm^{-1}), g-factor, paramagnetic impurities x and temperature independent paramagnetism (10^{-6} cm^3/mol) for dimeric and tetrameric models.

Model	Dimer	Tetramer
J_{12}	−264 (±5)	−264 (±5)
J_{11}'		+2 (±4)
J_{12}'		+1 (±4)
J_{22}'		0 (fixed)
g-factor	2.20 (fixed)	2.20 (fixed)
x	0.0018	0.0018
N_α	77.8	77.7

The calculated susceptibility values from both models are in very good agreement so that the temperature dependence of the magnetic susceptibility can be described by the same calculated curve valid for dimeric and tetrameric molecules (see Fig. 5). The theoretical analysis assuming tetrameric interaction shows only very small exchange integrals as being responsible for interdimeric interaction. So we shall discuss the magnetic behaviour of an asymmetric bridged dimer and neglect the small interdimeric interaction.

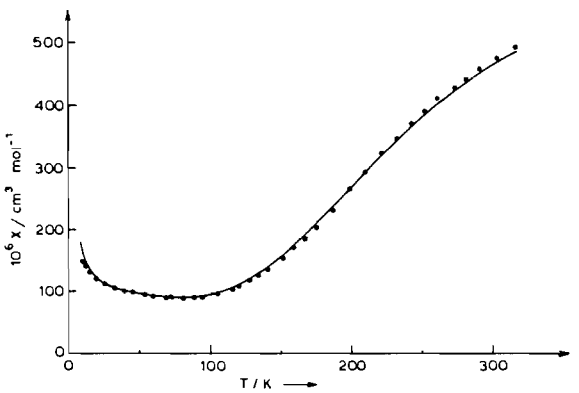

Fig. 5. Temperature dependence of the magnetic susceptibility. (●) Experimental and (–) calculated values using eqn. (3) for tetrameric as well as dimeric molecules.

The asymmetric bridged dimer has been characterized by an exchange coupling of $2J = -528$ cm^{-1}. The symmetry of the dimeric subunit containing an oxygen as well as a nitrogen as bridging ligands can be approached by C_s.

Comparison of the Cu–O–Cu angle of 102.9° with correlations for di-oxygen bridged dimers results in $2J$-values of −400 cm^{-1} and −620 cm^{-1} assuming the Hatfield-correlation for di-hydroxo bridged systems [12] and the Merz-correlation for di-alkoxo bridged complexes [13], respectively.

On the other hand di-azido bridged dimers having a Cu–N–Cu bridging angle of 104.5° were assumed to be coupled ferromagnetically [18]. So it was supposed that decreasing electronegativity of the bridging ligand results in a diminution of the antiferromagnetic part of the exchange coupling involving the same bridging angle.

In fact the mixed bridged systems cannot be compared with the symmetric ones because of the different symmetry of the magnetic orbitals. So C_s-symmetry leads to a_1- and a_2-type orbitals compared with the b_{1g}- and b_{2u}-types for D_{2h}-symmetry assumed for symmetric bridged dimers. A comparison of the energy dependence of the magnetic molecular orbitals is not possible. But the difference between the energy levels S = 0 and S = 1 has approximately the same magnitude as has been found for the di-oxygen bridged dimers.

Infrared Spectra

IR spectra are sometimes used to discuss azido-bonding in metallo-proteins such as met-azido-hemocyanin and in related metal complexes to distinguish between $\mu(1)$ and $\mu(1,3)$ bridging. Strong IR absorptions due to the $\nu_{asym}(N_3)$-vibration are observed for the discussed complex at 2095 and 2045 cm^{-1} including a shoulder at 2060 cm^{-1}. As is known from other azido-ligated metal complexes [31, 32] the energy of $\nu_{asym}(N_3)$ is shifted to higher values by increasing the difference Δd between the two N–N-distances. So a linear correlation between $\nu_{asym}(N_3)$ and Δd has been found [31]. Comparison of the N–N-distances in Table III results in symmetry within experimental error for the terminal and the $\mu_2(1)$-bridging azido-groups and in a Δd-value of 0.058(26) for the $\mu_3(1)$-bridging one. The position of the $\nu_{asym}(N_3)$ vibration at 2095 cm^{-1} can be explained by the increasing degree of asymmetry of the $\mu_3(1)$ azido-group. The vibrations at 2045 and 2060 cm^{-1} can be correlated with the two symmetric end-on bound azido-groups.

So IR spectroscopy seems not to be diagnostic of the mode of azide co-ordination because the ν_{asym} vibration for symmetric $\mu(1,3)$-bridging azides has

been found in the region of 2020–2050 cm^{-1} [8, 35, 36] similar to the end-on bound azido-groups in the discussed complex.

Conclusion

Some aspects of the binuclear copper site in hemocyanin are still unknown. So no interpretation of the magnetic behaviour in terms of assumed asymmetric bridging and of the large bridging angle at the endogenous ligand can be given.

Molecules modeling the hemocyanin active site are rare. But examination of dimeric units approaching one of the properties of the binuclear enzymatic complex (bridging angle, asymmetric bridges) can help to give an idea of magnetic exchange coupling in hemocyanin. In our opinion the discussed binuclear subunit is a good first example to understand more of the magneto-structural properties of the binuclear Cu(II)-unit in the diamagnetic oxy- and met-hemocyanins. But it is necessary to describe more asymmetric bridged dimers in a large angle region to establish a correlation between exchange coupling and bridging angle involving different asymmetric bridges. Then it might be possible to describe the role of magnetic exchange coupling in hemocyanin.

Acknowledgements

This work has been supported by the Deutsche Forschungsgemeinschaft. J. L. thanks the Fond der Chemischen Industrie, Frankfurt for a scholarship.

References

1 E. I. Solomon, in T. G. Spiro (ed.), 'Metal Ions in Proteins, Vol. 3', Wiley-Interscience, New York, 1981, p. 41.
2 T. B. Freedman, J. S. Loehr and T. M. Loehr, *J. Am. Chem. Soc., 98,* 2809 (1976).
3 J. A. Larrabee and T. G. Spiro, *J. Am. Chem. Soc., 102,* 4217 (1980).
4 N. C. Eickman, R. S. Himmelwright and E. I. Solomon, *Proc. Nat. Acad. Sci. U.S.A., 76,* 2094 (1979).
5 R. S. Himmelwright, N. C. Eickman, C. D. LuBien and E. I. Solomon, *J. Am. Chem. Soc., 102,* 5378 (1980).
6 G. L. Woolery, L. Powers, M. Winkler, E. I. Solomon and T. G. Spiro, *J. Am. Chem. Soc., 106,* 86 (1984).
7 D. M. Dooley, R. A. Scott, J. Ellinghaus, E. I. Solomon and H. B. Gray, *Proc. Nat. Acad. Sci. U.S.A., 75,* 3019 (1978).
8 V. McKee, J. V. Dagdigian, R. Bau and C. A. Reed, *J. Am. Chem. Soc., 103,* 7000 (1981).
9 P. K. Coughlin and S. J. Lippard, *J. Am. Chem. Soc., 103,* 3228 (1981).
10 P. L Burk, J. A. Osborn, M.-T. Youinou, Y. Agnus, R. Louis and R. Weiss, *J. Am. Chem. Soc., 103,* 1273 (1981).
11 M. S. Haddad, W. R. Wilson, D. J. Hodgson and N. D. Hendrickson, *J. Am. Chem. Soc., 103,* 384 (1981).
12 W. E. Hatfield, in E. A. Boudreaux and L. N. Mulay (eds.), 'Theory and Applications of Molecular Paramagnetism', Wiley-Interscience, New York, 1976.
13 L. Merz and W. Haase, *J. Chem. Soc., Dalton Trans.,* 875 (1980).
14 R. Robson, *Inorg. Nucl. Chem. Letters, 6,* 125 (1970); R. Robson, *Aust. J. Chem., 23,* 2217 (1970).
15 H. Okawa, T. Tokii, Y. Nonaka, Y. Muto and S. Kida, *Bull. Chem. Soc. Jpn., 46,* 1462 (1973).
16 R. J. Majeste, C. L. Klein and E. D. Stevens, *Acta Crystallogr., Sect. C:, 39,* 52 (1983).
17 K. D. Karlin, J. C. Hayes, J. P. Hutchinson and J. Zubieta, *J. Chem. Soc., Chem. Commun.,* 376 (1983).
18 J. Comarmond, P. Plumeré, J.-M. Lehn, Y. Agnus, R. Louis, R. Weiss, O. Kahn and I. Morgenstern-Badarau, *J. Am. Chem. Soc., 104,* 6330 (1982).
19 C. G. Barraclough, R. W. Brookes and R. L. Martin, *Aust. J. Chem., 27,* 1843 (1974).
20 F. Ullmann and K. Brittner, *Ber. Dtsch. Chem. Ges.,* 2539 (1909).
21 P. Main, S. J. Fiske, S. E. Hull, L. Lessinger, G. Germain, J.-P. Declercq and M. M. Woolfson, 'MULTAN 80', A System of Computer Programs for the Automatic Solution of Crystal Structures from X-Ray Diffraction Data. Universities of York and Lourain, 1980.
22 'International Tables for X-Ray Crystallography, Vol. IV', Kynoch Press, Birmingham, 1973, p. 99, 149.
23 D. T. Cromer and J. B. Mann, *Acta Crystallogr. Sect. A:, 24,* 321 (1968).
24 L. Merz, *Dissertation,* Technische Hochschule Darmstadt, 1980.
25 A. Weiss and H. Witte, "Magnetochemie", Verlag Chemie, Weinheim, 1973.
26 J. E. Andrew and A. B. Blake, *J. Chem. Soc., Dalton Trans.,* 1102 (1973).
27 B. F. Hoskins, R. Robson and D. Vince, *J. Chem. Soc., Chem. Commun.,* 392 (1973).
28 M. R. Churchill and B. G. DeBoer, *Inorg. Chem., 14,* 2502 (1975).
29 W. Mazurek, K. J. Berry, K. S. Murray, M. J. O'Connor, M. R. Snow and A. G. Wedd, *Inorg. Chem., 21,* 3071 (1982).
30 M. A. S. Goher and T. C. W. Mak, *Inorg. Chim. Acta, 85,* 117 (1984).
31 I. Agrell, *Acta Chem. Scand., 25,* 2965 (1971).
32 Z. Dori and R. F. Ziolo, *Chem. Rev., 73,* 247 (1973).
33 W. E. Hatfield and G. W. Inman, *Inorg. Chem., 8,* 1376 (1969).
34 B. Bleaney and K. D. Bowers, *Proc. R. Soc., A214,* 451 (1952).
35 Y. Agnus, R. Louis and R. Weiss, *J. Am. Chem. Soc., 101,* 3381 (1979).
36 R. F. Ziolo, A. P. Gaughan, Z. Dori, C. G. Pierport and R. Eisenberg, *Inorg. Chem., 10,* 1289 (1971).